ICWE14
June 21-26, 2015 | Porto Alegre - Brazil
14th INTERNATIONAL CONFERENCE ON WIND ENGINEERING

Experimental investigation of low-frequency turbulence effects on the aeroelastic response of model-scale long span bridge

T. Argentini[1], G. Diana[1], D. Rocchi[1], C. Somaschini[1]
[1]Department of Mechanical Eng., Politecnico di Milano, Milan, Italy
email: tommaso.argentini@polimi.it, giorgio.diana@polimi.it, daniele.rocchi@polimi.it, claudio.somaschini@polimi.it

ABSTRACT: The influence of the low frequency turbulence components on the response of long span bridges was studied through experimental tests performed on a full bridge aeroelastic model in the wind tunnel of the Politecnico di Milano using an active turbulence generator able to generate a correlated deterministic harmonic turbulence. The experimental evidence underlined the nonlinear effect of the low frequency incoming turbulence on the dynamic high frequency response of the structure. Therefore, numerical simulations are used to explain the bridge behavior considering the variation of the aeroelastic properties of the bridge with the instantaneous angle of attack and reduced velocity.

Even though the wind tunnel experiment uses an oversimplified wind spectrum with an intentionally high correlation along the main span, it helps to understand the nonlinear interaction between the low frequency and the high frequency buffeting response.

KEY WORDS: wind tunnel; aeroelastic model; long span bridge; band superposition; buffeting; aeroelasticity.

1 INTRODUCTION

In bridges aerodynamics, the modeling of non-linearities of wind loads acting on deck is still an open issue. Among the numerical models, the Band Superposition approach (BS) [5], [6], [7], [9], [10] is a well-established procedure to account for nonlinear aerodynamic effects, exploiting the knowledge of static coefficients, flutter derivatives, and admittance functions, as a function of the reduced velocity and of the mean angle of attack.

The BS approach relies on the assumption that nonlinear effects, acting at low frequency (LF band), are mainly induced by the large fluctuation of the instantaneous angle of attack produced by LF turbulence, while the nonlinear effects at high frequency (HF band) may be modeled by a linearized approach around the LF band solution. In the HF band, the dependence on both the reduced velocity and the angle of attack is taken into account through a numerical model whose coefficients change in time, while for the LF band a corrected quasi-steady approach is used [2]. Furthermore, in the real situations, turbulent wind with integral length scale of hundreds of meters and large LF fluctuations have been measured by different experimental campaign [4], [12].

Even though experimental validations of the BS approach are proposed by means of wind tunnel tests on sectional deck models both using forced motion or elastically suspended set ups, no evidence are present in literature on full aeroelastic models.

In this paper, we present the experimental results of a wind tunnel campaign performed on an aeroelastic model of long span-bridge (1:220 scale) aimed at highlighting the effects of LF incoming turbulence on the dynamic HF response of the structure. To this end, an active turbulence generator was used to generate a correlated deterministic harmonic turbulence. The active turbulent generator is able to produce a multi-harmonic perturbation of the flow with a strongly correlated vertical component of the wind velocity.

The response of the structure was recorded under two different incoming flow conditions: a) HF turbulent component only; b) HF turbulence modulated by a LF component. Comparing the high frequency responses of the bridge in the two different cases, it is possible to highlight the interaction effects of the LF incoming turbulence that can be analyzed and explained using numerical models. Indeed, numerical simulations are performed in order to explain the different aeroelastic behavior of the bridge: an eigenvalue-eigenvectors analysis of the aeroelastic system is performed to show the effect of the dependence of aerodynamic forces on the LF instantaneous angle of attack and reduced velocity. Furthermore, a BS simulation in the time domain is performed to highlight the method capability to reproduce the strongly non-linear aeroelastic response.

2 EXPERIMENTAL SETUP

2.1 Aeroelastic model of the bridge

The bridge studied in the present research is the Izmit Bay Bridge, a three spans suspension bridge with a main central span of 1550 m and two side spans of 566 m. Each tower is a 235.43 m high steel structure having two crossbeams connecting the two tower legs at the middle level and at the top. The towers foundations are placed on the gravel bed, at 40 m below water level. The main cables are deviated at the side span piers and anchored at the cable anchor blocks. The deck is a classical streamlined single

box (characterized by a three-lane dual carriageway with no railway), 31.5 m wide and 4.75 m deep, having 2.8 m wide inspection walkway on both sides. The general arrangement of the bridge is shown in Fig. 1, while the deck cross-section is shown in Fig. 2. Aeroelastic tests were performed on an aeroelastic model of the full bridge in the Boundary Layer Wind Tunnel of Politecnico di Milano (Figure 3). The model was realized in a 1:220 geometrical scale, using Froude similarity [11].

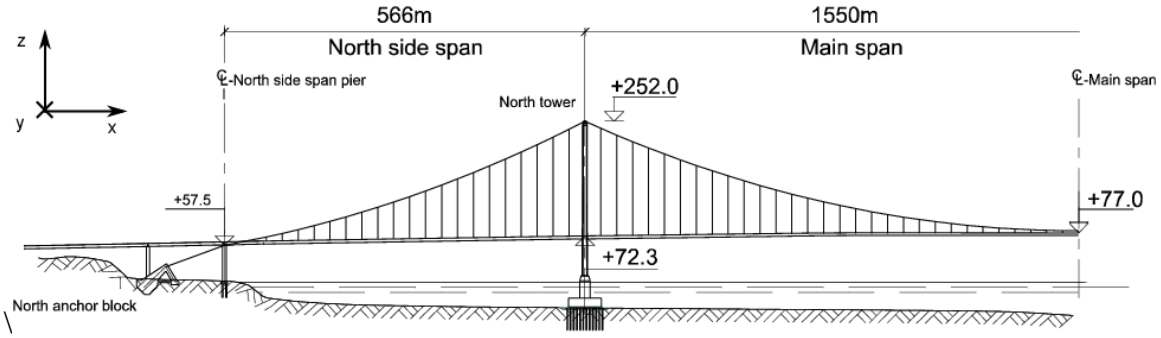

Figure 1. General arrangement of the bridge.

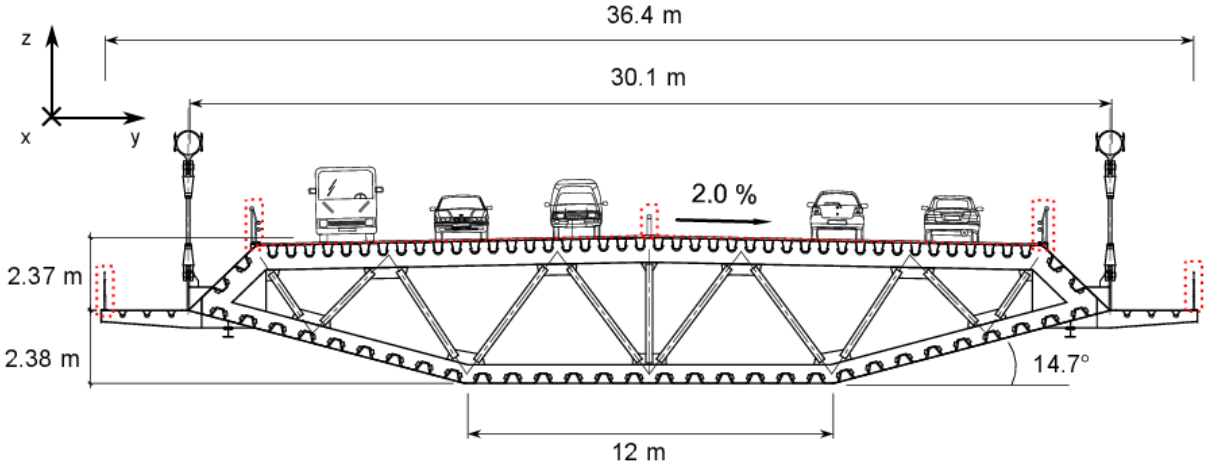

Figure 2. Typical deck cross section overall dimensions.

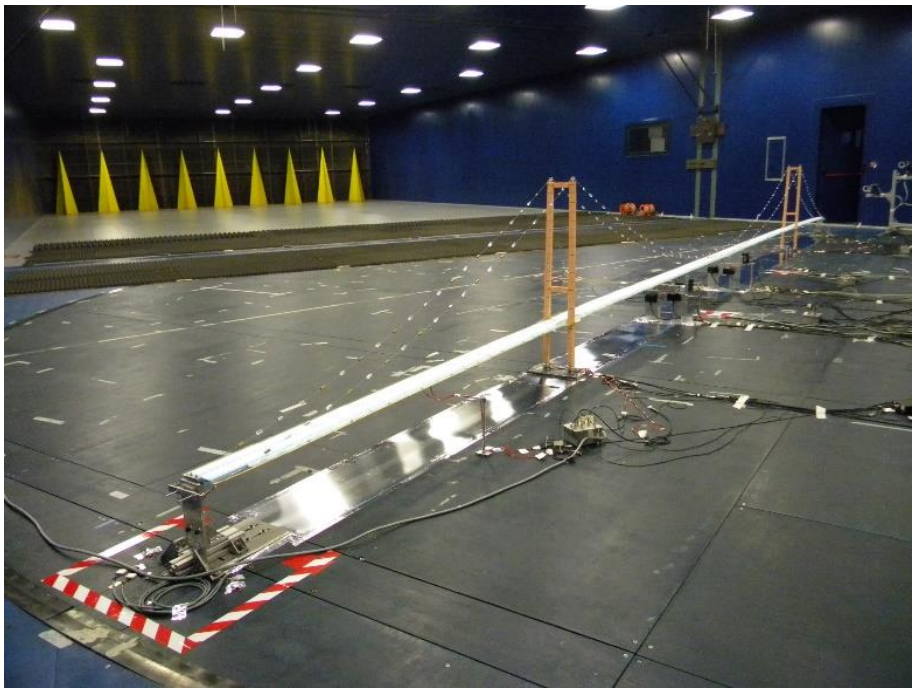

Figure 3. The full bridge aeroelastic model in the boundary layer wind tunnel.

2.2 Aerodynamic coefficients

The aerodynamic static coefficients of the deck were measured on a sectional model with the same geometrical scale of the full-bridge, using the test rig shown in Figure 4. With the same experimental setup, also the self-excited torsional unsteady aerodynamic terms of lift and moment acting on the deck section (flutter derivatives $a^*_{2,3}$, $h^*_{2,3}$, $p^*_{2,3}$) were measured, using a forced motion technique. The other unsteady aerodynamic coefficients used in the simulations were inferred from their quasi-steady values.

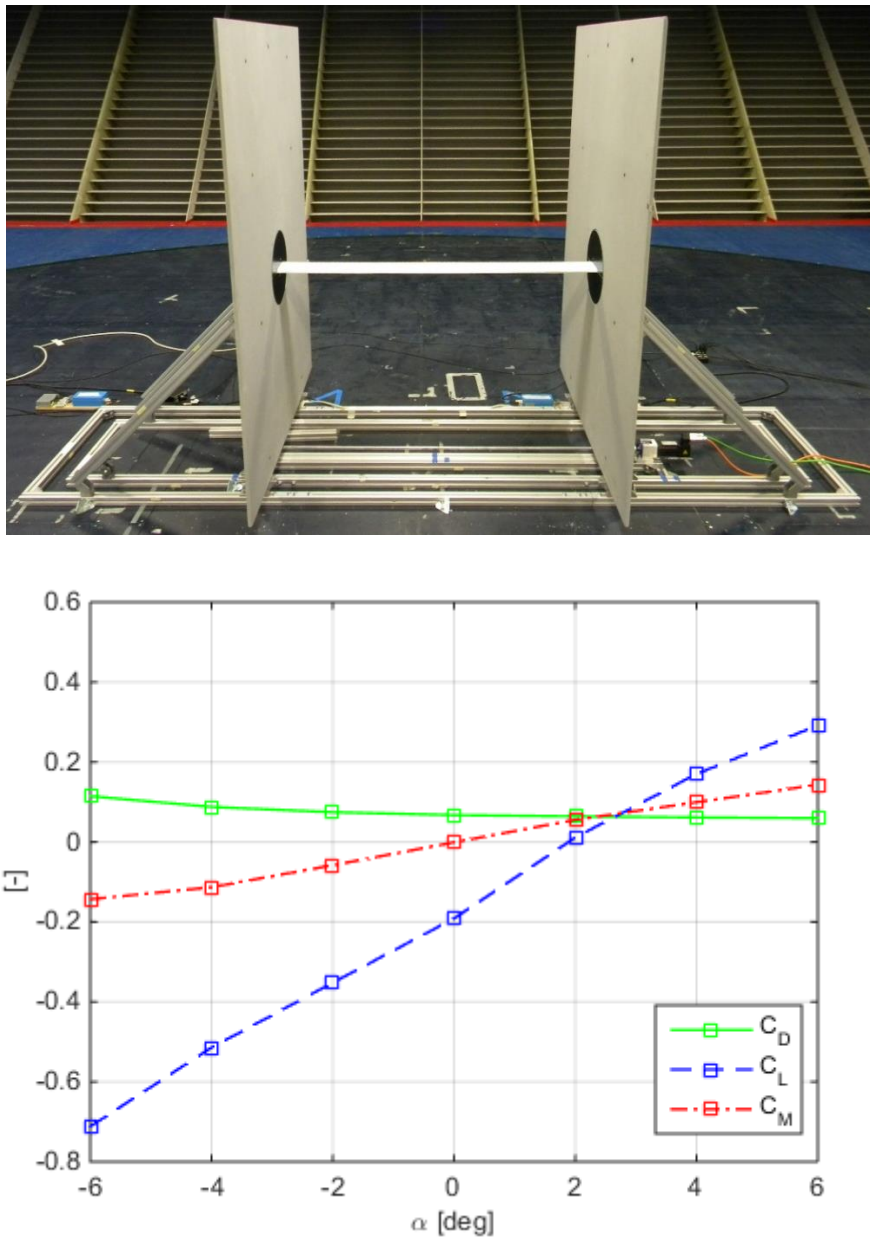

Figure 4. Experimental setup for measuring flutter derivatives and static coefficients on the deck sectional model (in 1:220 scale).

2.3 Active turbulence generator

An active turbulence generator, made by a vertical array of 10 NACA 0012 airfoils, 4 m wide, is used to generate a harmonic wind wave [10]. The airfoils are driven by two brushless motors giving a pitching motion according to a user-defined motion law in terms of frequency contents and amplitude (Figure 4). The turbulence generator is positioned 7 m upwind the model, while the incoming wind is measured one chord before the leading edge by means of a 4-holes probe that resolves the instantaneous vertical and horizontal wind components. The coherent wave has a width of 4m compared to a main span of 7m and a total length of 12 m (Figure 6).

The airfoils deflect the incoming wind changing the angle of attack of the wind blowing in the bridge. Thus the instantaneous angle of attack α is sum of the deck rotation θ plus the LF wind angle β, as shown in Figure 7.

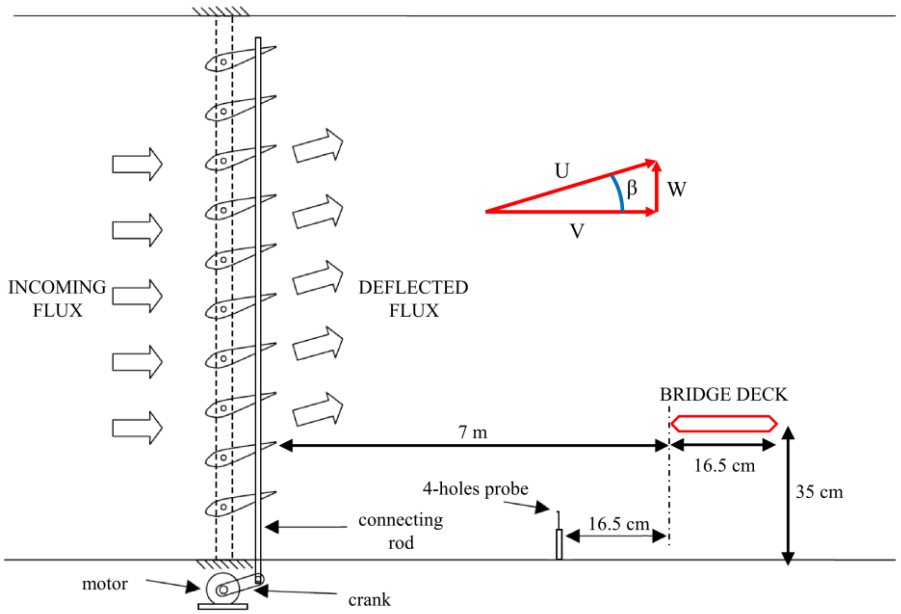

Figure 5. Active turbulence generator, lateral view.

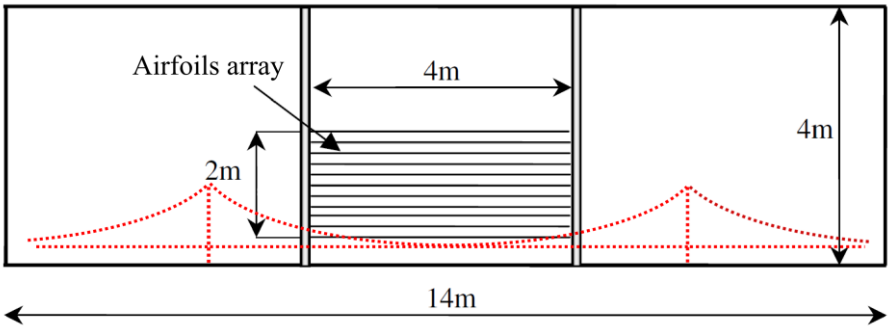

Figure 6. Active turbulence generator, frontal view.

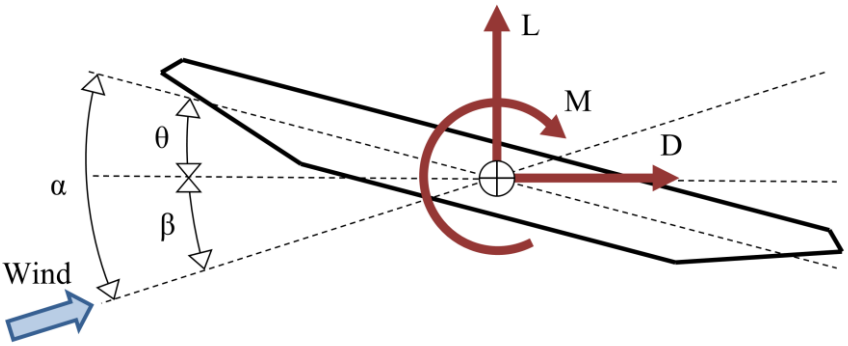

Figure 7. Conventions for the angles.

2.4 Structural modes

Since the turbulence generator is placed in the central section of the main span the modes forced by the coherent fluctuations are mainly the symmetrical ones with respect to the center of the bridge. During the test campaign also a study on the flutter instability of the bridge has been carried out discovering a critical speed of 5.53 m/s and a flutter frequency of 2.57 Hz. The structural modes mainly involved in the flutter are the first and the fifth vertical bending and the first torsional one. The natural frequencies of these modes are 1.31 Hz, 2.87 Hz and 3.84 Hz respectively while their modal shapes are reported in Figure 8.

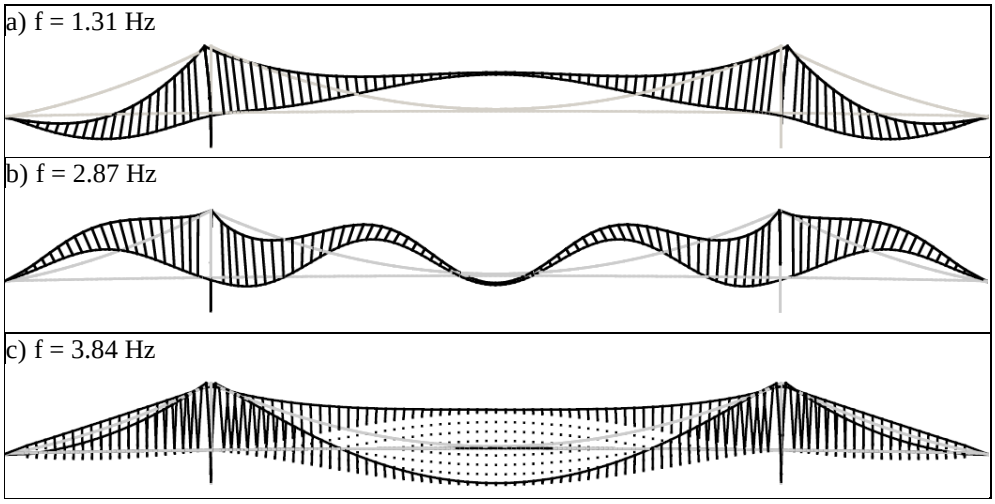

Figure 8. Modal shapes of the first vertical bending modes (above) and of the first torsional mode (below).

3 EXPERIMENTAL RESULTS

Two different wind tunnel tests were performed with a mean wind velocity of 5 m/s to investigate the effects of low-frequency coherent fluctuations of the incoming turbulent wind (angle of attack):

Case a) single-harmonic vertical turbulence with a HF component at 2.57 Hz (reduced velocity $V^* = V/(fB) = 12$) with small amplitude ($\beta = 1$ deg) representing a contribution of the high frequency part of the wind spectrum;

Case b) double-harmonic vertical turbulence with a HF component at 2.57 Hz with small amplitude ($\beta = 1$ deg) + LF component at 0.1 Hz (reduced velocity $V^* = 31$) with amplitude $\beta_{LF} = 2$ deg, representing two contributions of the wind spectrum.

The choice of 5 m/s for the mean wind speed was done in order to have a strong aerodynamic coupling between modes; the forcing frequency at 2.57 Hz is a frequency near the eigen-frequencies of the aeroelastic system at 5 m/s, and it forces efficiently the symmetric modes.

3.1 Flow generated

The angle of attack measured by the multi-hole probes at deck height in both cases are shown in Figure 9 and Figure 10 in terms of spectra.

In the first case, as expected, the flow is characterized by a constant horizontal mean component with a vertical high frequency component of 2.57 Hz. On the other hand, with regard to the second case, the low frequency contents are clearly visible but the high frequencies have some sub- and super- harmonics, probably due to a floor effect. However, in the authors' opinion, this boundary effect can be neglected with regard to the results presented in this paper.

The same results shown in Figure 10 are visible in a graphical manner in Figure 11. This figure shows two frames of the smoke visualization of the flow; in this way it is possible to see the two different wavelengths of the low and high frequency components of the vertical velocity.

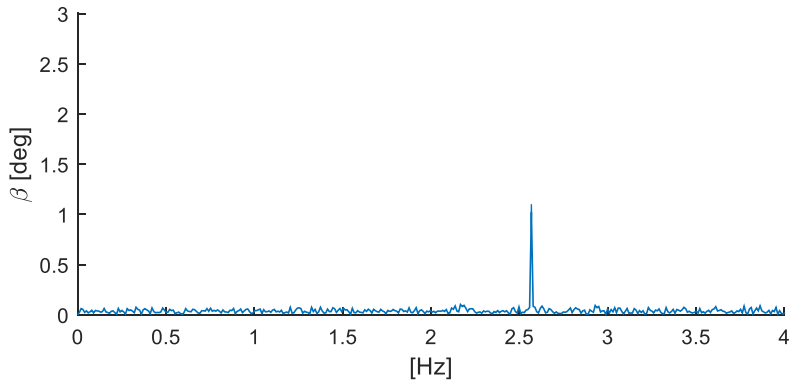

Figure 9. Time evolution and spectra of the components of the flow generated in the case *a*.

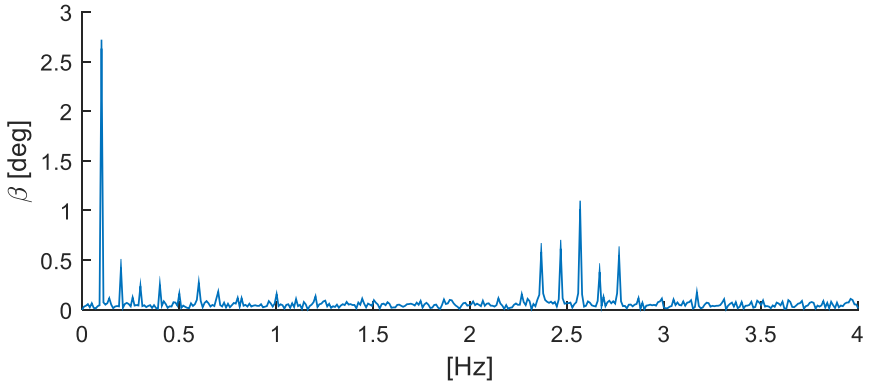

Figure 10. Time evolution and spectra of the components of the flow generated in the case *b*.

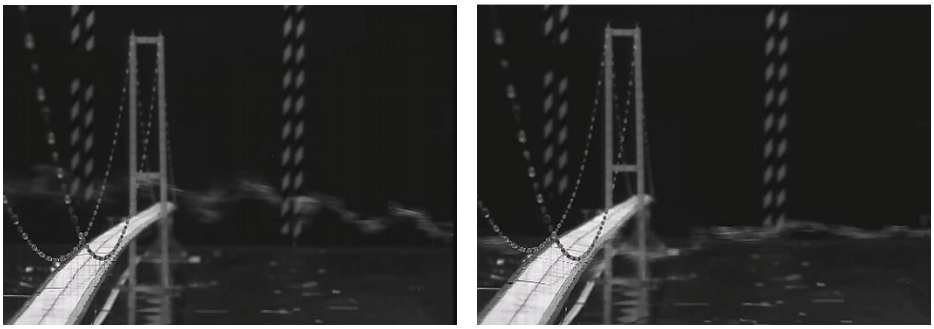

Figure 11. Two frames of the smoke visualization of the flux turbulence: upward flow (left) and downward flow (right).

3.2 Bridge response

Figure 12 and Figure 13 show the recorded vertical accelerations at mid-span overlapped to the low-frequency time evolution of the angle of attack β_{LF} due to turbulence. Looking at the time histories of the response in case *b*, it is possible to notice that the HF dynamic response is strongly dependent on the LF incoming turbulence. In particular, in correspondence with negative LF angles of attack generated by the turbulence the deck response is more than twice the reference case *a*. This result shows that, although in the two cases the mean speed and the high frequency contents are almost the same, the bridge reacts in two very different ways depending on the velocity angle given by the low frequency component. In this case, the total angle of attack is the deck rotation θ (static + LF) in addition to the wind angle β_{LF}.

This behavior can be explained looking at the dependence of the unsteady aerodynamic coefficients upon the mean angle of attack. Considering that the static rotation of the deck is 2 degrees nose up at 5 m/s, the angle of attack in case b oscillates at least between 4 and 0 degrees (plus the θ_{LF} , whose values are not available). On the other hand the mean wind speed is steady, this means that the reduced speed does not change between the two cases, and it is possible to study the trend of the flutter derivatives as a function of the angle of attack, as shown in Figure 14. The comparison shows that the aerodynamic coefficients more influenced by the angle are a_2^* and h_2^*. Specifically a_2^*, that is the coefficient related to the aerodynamic torsional damping[1], decreases at 4 degrees.

[1] Considering the convenctions propoposed by Zasso [13] $M = -\frac{1}{2}\rho V^2 B^2 a_2^* \frac{B\dot{\theta}}{V}$, therefore a positive a_2^* corresponds to a positive aerodynamic damping

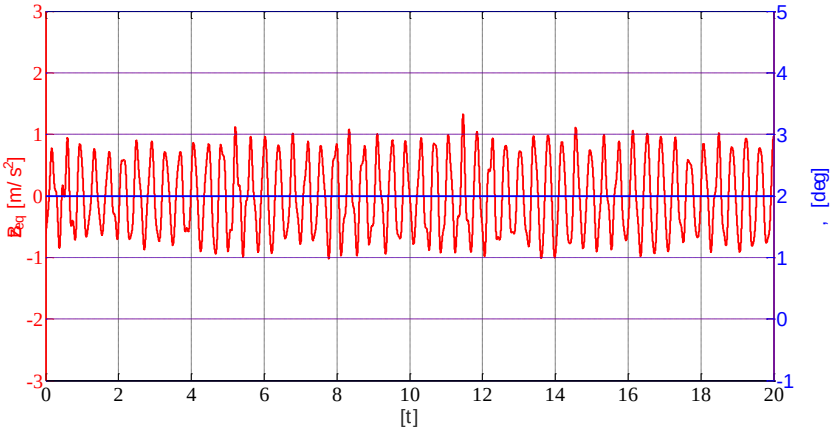

Figure 12. Comparison of torsional mode response in case a: $f_{HF} = 2.57$ Hz. Reported values are equivalent torsional accelerations at deck edge $\ddot{z}_{eq} = \ddot{\theta}B/2$. The blue line represents the LF angle of the incoming wind β_{LF}.

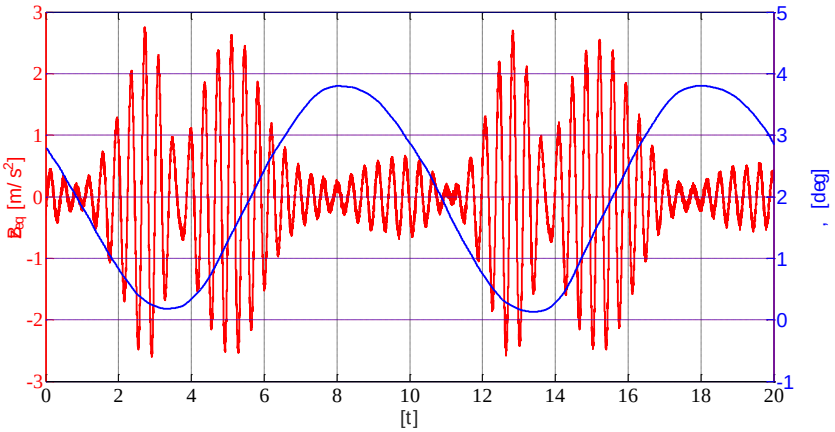

Figure 13. Comparison of torsional mode response in case b: $f_{LF} = 0.1$ Hz + $f_{HF} = 2.57$ Hz. Reported values are equivalent torsional accelerations at deck edge $\ddot{z}_{eq} = \ddot{\theta}B/2$ .The blue line represents the LF angle of the incoming wind β_{LF}.

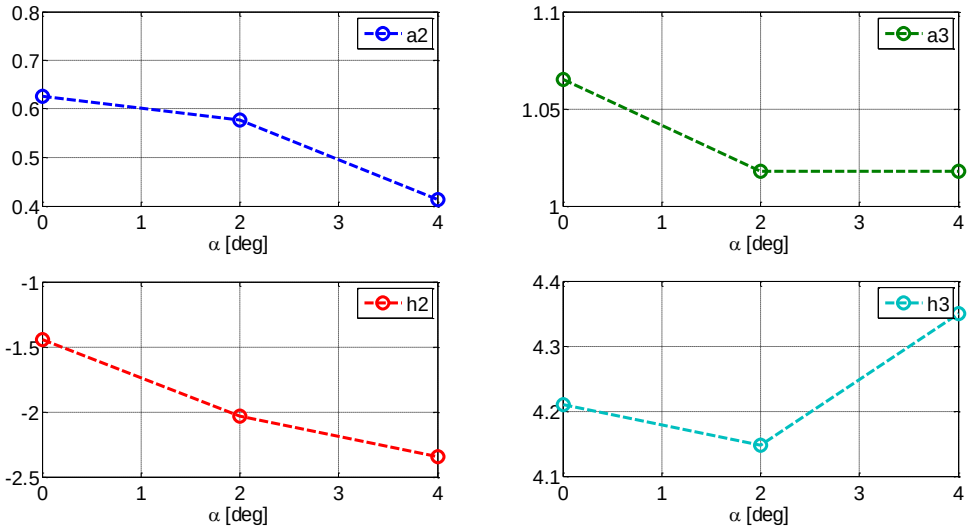

Figure 14. Trend of the flutter derivatives at a fixed V^* of 12 as a function of the angle of attack.

4 NUMERICAL RESULTS

4.1 Eigenvalue-eigenvector analysis

Starting from the results of the experimental campaign, a numerical study was carried out in order to investigate the effect different angles of attack on the aeroelastic coupling of the bridge, and specifically on its eigenvalues/eigenvectors. The used algorithm is based on multi-modal equations and solves the eigenvalues problems of the interaction between wind and structure at different speed [3]. In the simulations, three symmetric modes were used: the first and the fifth vertical bending mode and the first torsional mode; which are the most important modes as regard to the flutter instability [1]. In Figure 15 the damping evolution of the reference case, with $\alpha = 2$ deg, is reported as a function of the wind speed; in this case the wind angle β is zero and the angle of attack is only function of the static coefficient C_M (Figure 16). The critical speed is around 5.8 m/s while the lowest damping at 5 m/s is the one of the second mode of about 0.04.

Other two simulations have been done, adding and subtracting 2 degrees to the angle of attack, as if the LF fluctuation where steady. The results obtained are shown in Figure 17 compared to the reference case. From this figure is clearly visible that the second mode, with an angle of attack of 4 deg (2 deg of the static angle plus 2 deg of the incoming wind), has a very low damping in the speed range between 4.5 m/s and 5 m/s (≈ 1%). On the other hand, the same mode in the simulation with an angle of attack equal to zero has more or less the same damping of the reference case (≈ 4.5%). This means that the variation of the angle of attack, fixed in the simulations while given by the low frequency fluctuation in the real situation, shift the eigenvalues of the system from a stable condition to a more unstable condition as it was seen in the experimental tests.

To be thorough, in Figure 18 the magnitudes and the phases of the eigenvectors at 5 m/s of the mode "1T" are shown. From the comparison, remarkable differences between the modes shapes are not highlighted but, on the contrary, they are comparable, therefore we can say that the different total damping is linked to the direct aerodynamic damping and not to a different coupling of mode shapes.

4.2 Band Superposition simulation

The behavior of the bridge has also been simulated with a Band-Superposition model [10] applied to the full bridge. The algorithm flow-chart of the BS approach is reported in Figure 19, and the procedure consists of three main steps:

LF-HF threshold definition → LF response computation → HF response computation

The LF-HF threshold has to be defined in terms of reduced velocity V^* or reduced frequency f^*. This threshold delimits the region where the flutter derivatives and the aerodynamic admittance functions show small dependence on the reduced velocity. For the considered case, the LF vertical wind speed component is mono-harmonic at 0.1 Hz (V^*=31) with amplitude β = 2 deg; the LF computation is simulated using a nonlinear corrected quasi-steady theory (e.g. [9], [10]).

The HF band solution can be simulated with a rheological numerical model [10] or with a multi-band approach [8]. Both approaches model HF forces with parameters that are modulated by the instantaneous LF angle of attack: self-induced and buffeting forces are computed independently and their effect are summed up exploiting the superposition hypothesis. In the considered test case the central part of the mid-span is forced by a turbulent vertical wind component at 2.57 Hz (V*=12) with amplitude β = 1 deg. The lateral spans are forced by a laminar wind.

Figure 20 shows the simulated time history at the mid-span section (to be compared with Figure 13). We can highlight that the effect of the LF angle of attack is well reproduced: in particular there is an amplification of the response for positive α, and a reduction for negative α. The maximum vibration levels, for the equivalent acceleration at deck edge, are in both cases about 3 m/s^2.

5 CONCLUSIONS

This research adds a contribution in the analysis of the non-linear effects on the buffeting response induced by the variation of the instantaneous angle of attack produced by the LF contribution of turbulence in the incoming flow.

An experimental evidence of the aeroelastic interaction between the low frequency fluctuation of the instantaneous angle of attack induced by the turbulence and the corresponding high frequency response was presented in the paper. This experiment was focused on experimentally investigate the band superposition approach on a strongly coupled multimode full bridge.

Even if the wind spectrum was simplified, reproducing only two frequency components at LF and HF, and even if the spatial correlation is extremely large along the central span, the structural dynamics of the model and the aerodynamic coefficients of the deck are representative of real long span bridge. Therefore the dynamic response of the bridge is the result of both the aeroelastic coupling of structural modes and of the buffeting excitation.

Tests have been performed at high mean wind velocity in order to have a strong aeroelastic coupling between modes, but with realistic turbulent wind speed components (larger for LF terms and smaller for HF terms) and reduced velocities. The buffeting forces, acting along the central part of the main span (about 30% of its length) force efficiently the symmetric modes, since they

have a large lagrangian component. Moreover, the selection of a high frequency near to resonance allowed to highlight the bridge dynamics.

The bridge HF response shows highly nonlinear effects that may be explained analyzing the dependence of the flutter derivatives on the instantaneous angle of attack, at the considered V*. The low frequency angle of attack is the contribution of the LF turbulent wind plus the LF response of the deck (in particular of its rotation): both a simplified eigenvalue analysis and a more complex band superposition model were used to support this explanation. This test-case is another evidence that supports the need for a characterization of the deck unsteady aerodynamics in a large range of angles of attack also at low reduced velocities.

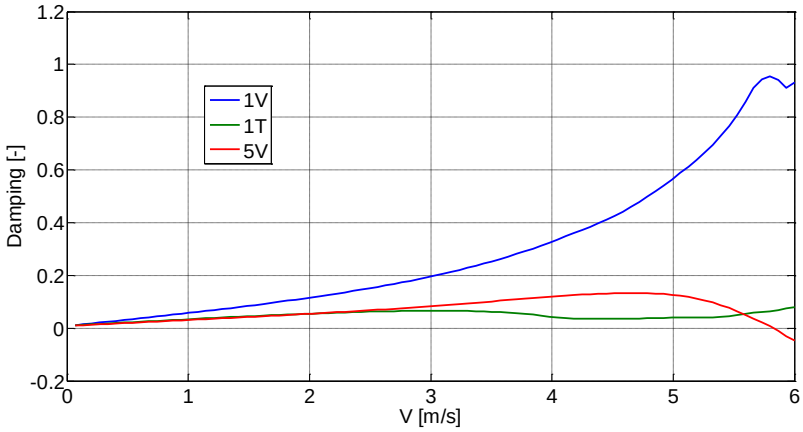

Figure 15. Evolution of the damping of the modes used in the eigenvalue analysis as a function of the incoming wind speed.

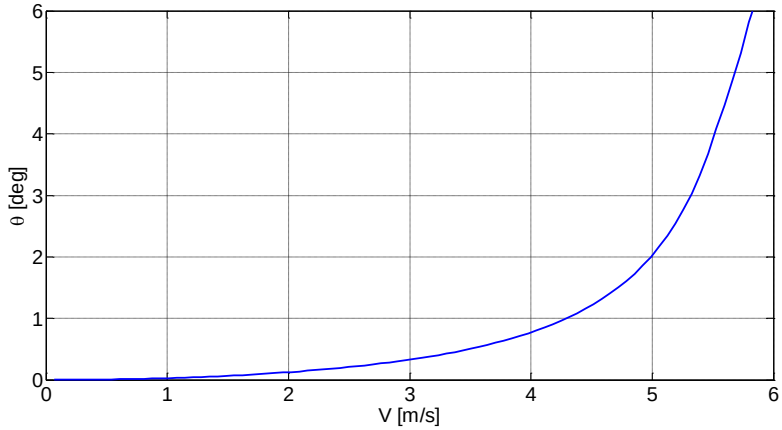

Figure 16. Static deck rotation at mid-span as a function of the incoming wind speed.

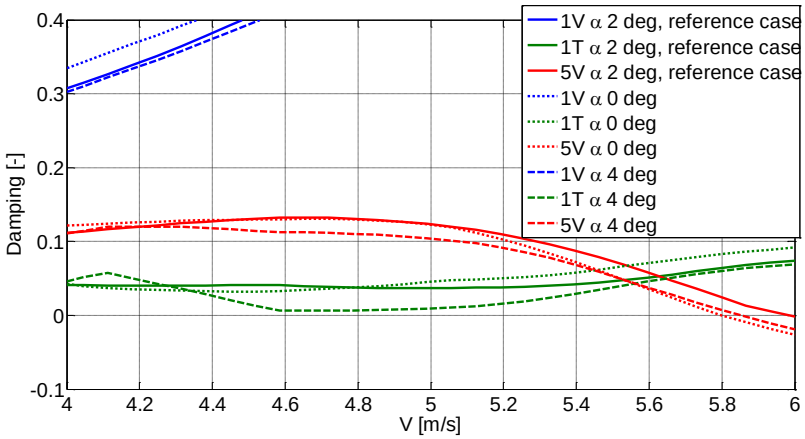

Figure 17. Damping of the three modes in the different simulations as a function of the incoming wind speed.

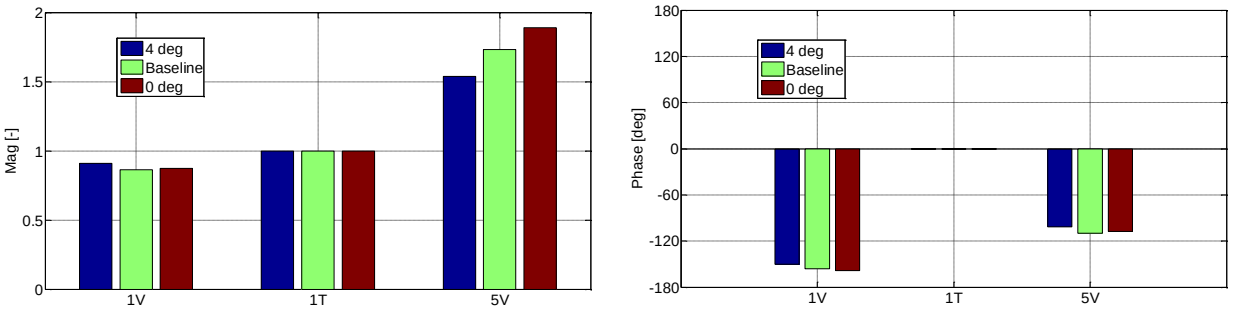

Figure 18. Magnitudes and phases of the eigenvectors of the mode "1T" at 5 m/s in the three simulations.

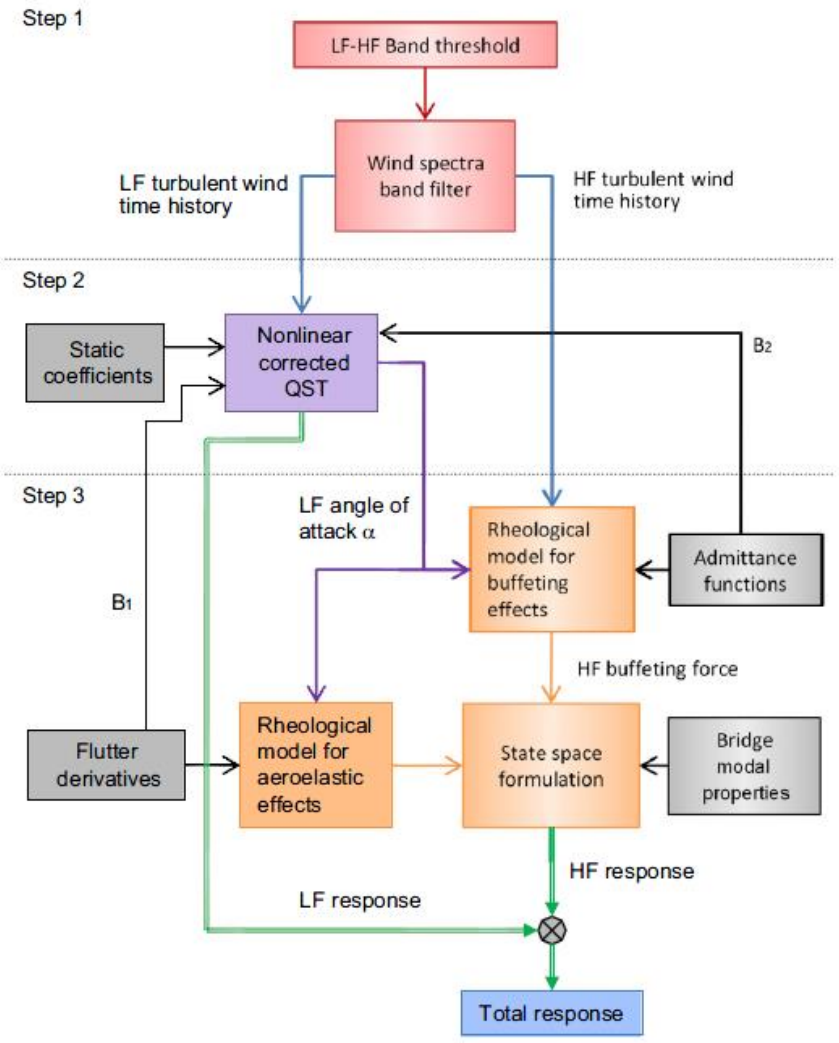

Figure 19. Band Superposition algorithm flow-chart (after [10]).

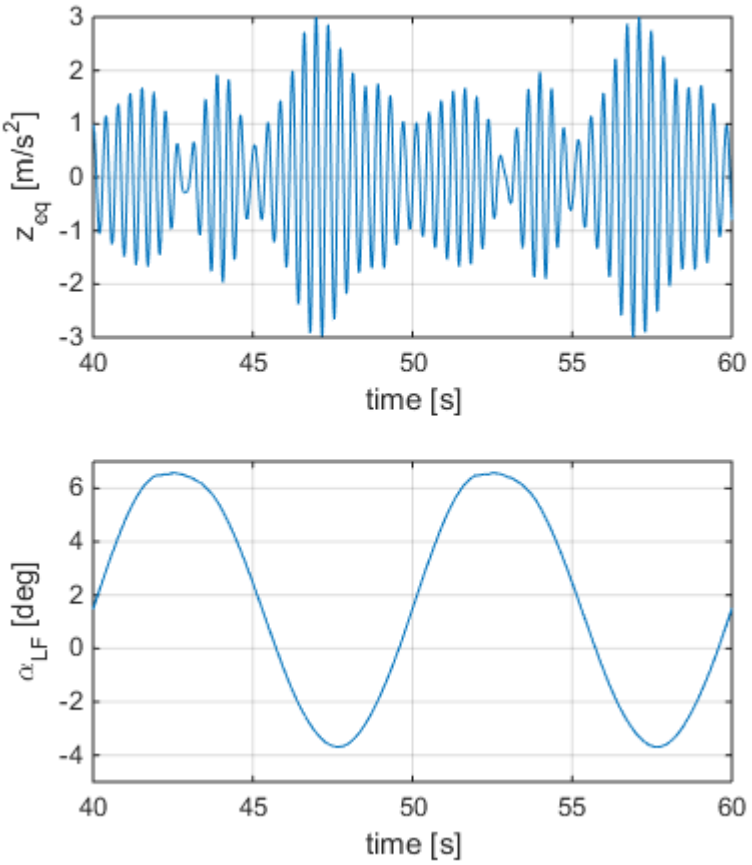

Figure 20. Band Superposition response: equivalent acceleration at deck edge in the mid-span section and corresponding LF angle of attack

REFERENCES

[1] Argentini, T., Diana, G., Larsen, A., Pagani, A., Portentoso, M., Somaschini, C., Yamasaki, Y., Comparisons between wind tunnel tests on a full aerolastic model and numerical results of the Izmit Bay Bridge. EACWE 2013: 6th European and African Conference on Wind Engineering, 2013.

[2] Argentini, T., Diana, G., Portentoso, M., Rocchi, D., Nonlinear buffeting response of bridge deck using the Band Superposition approach: comparison between rheological models and convolution integrals. CWE2014: 6th International Symposium on Computational Wind Engineering, 2014.

[3] Argentini, T., Pagani, A., Rocchi, D., Zasso, A., Monte Carlo analysis of total damping and flutter speed of a long span bridge: Effects of structural and aerodynamic uncertainties. Journal of Wind Engineering and Industrial Aerodynamics 128, 90 – 104, 2014.

[4] Bocciolone, M., Cheli, F., Curami, A., Zasso, A., Wind measurements on the Humber bridge and numerical simulations. Journal of Wind Engineering and Industrial Aerodynamics 42, 1393 – 1404, 1992.

[5] Chen, X., Kareem, A., Nonlinear response analysis of long-span bridges under turbulent winds. J. Wind Eng. Ind. Aerodyn. 89, 1335 – 1350, 2001.

[6] Chen, X., Kareem, A., Aeroelastic analysis of bridges: Effects of turbulence and aerodynamic nonlinearities. Journal of Engineering Mechanics 129, 885 – 895, 2003.

[7] Chen, X., Matsumoto, M., Kareem, A., Time domain flutter and buffeting response analysis of bridges. Journal of Engineering Mechanics 126, 7 – 16, 2000.

[8] Diana, G., Bruni, S., Rocchi, D., A numerical and experimental investigation on aerodynamic non linearities in bridge response to turbulent wind. EACWE 2005 - 4th European and African Conference on Wind Engineering 86 – 87, 2005.

[9] Diana, G., Falco, M.; Bruni, S., Cigada, A., Larose, G., Damsgaard, A. & Collina, A., Comparisons between wind tunnel tests on a full aeroelastic model of the proposed bridge over Stretto di Messina and numerical results Journal of Wind Engineering and Industrial Aerodynamics 54-55, 101 – 113, 1995.

[10] Diana, G., Rocchi, D., Argentini, T., An experimental validation of a band superposition model of the aerodynamic forces acting on multi-box deck sections. Journal of Wind Engineering and Industrial Aerodynamics 113, 40 – 58, 2013.

[11] Diana, G., Yamasaki, Y., Larsen, A., Rocchi, D., Giappino, S., Argentini, T., Pagani, A., Villani, M., Somaschini, C., Portentoso, M., Construction stages of the long span suspension Izmit Bay Bridge: Wind tunnel test assessment. Journal of Wind Engineering and Industrial Aerodynamics 123, 300 – 310, 2014.

[12] Hui, M.C.H., Larsen, A., Xiang, H.F., Wind turbulence characteristics study at the Stonecutters Bridge site: Part I-Mean wind and turbulence intensities. Journal of Wind Engineering and Industrial Aerodynamics 97, 22 – 36, 2009.

[13] Zasso, A., Flutter derivatives: Advantages of a new representation convention. Journal of Wind Engineering and Industrial Aerodynamics 60, 35 – 47, 1996.